Acta Cryst. (1992). A**48**, 842–850

Maximum-Entropy Method: Phase Refinement

BY TOMOHIRO SATO

Shionogi Research Laboratories, Shionogi & Co. Ltd, Fukushima-ku, Osaka 553, *Japan*

(*Received* 9 *December* 1991; *accepted* 11 *May* 1992)

Abstract

An algorithm is described for calculating the maximum-entropy (ME) electron density map that is constrained to satisfy each of the observed structure-factor amplitudes, *i.e.* $|F_h| - |F_h^{obs}| = 0$. The use of these phaseless constraints enables one to refine phases, and hence crystal structures, in terms of entropy. From the structure factors observed with a small molecule as well as values extrapolated from them, numerical calculations were done at various resolutions. The algorithm can be used to obtain atomic models even with 1.5 Å data, indicating that the ME method is a significant improvement over currently available direct methods. For practical purposes, the present algorithm may be used as an alternative to successive Fourier refinements following the initial stage of approximate phase determination.

Introduction

Various probabilistic approaches to the phase problem in crystallography have achieved remarkable success in elucidating the crystal structures of small molecules directly from observed X-ray data [for a review, see Woolfson (1987)]. These direct methods, however, are not effective for low-resolution structures with which fewer than half the theoretically measurable reflections in the range 1.1 to 1.2 Å are observable (Sheldrick, 1990). Thus, there has been much interest in the maximum-entropy (ME) method, which is believed to have the potential to expand the ability of current direct methods and to be applicable to such low-resolution structures as proteins (see, for example, Collins, 1982; Bricogne, 1984). The key principle in the ME method is simple and all that is required is to find the ME density distribution among those that are consistent with whatever data are available. Thus, there are several ways of using the method in crystallography depending on the choice of which data and information are to be used. Thus far, the ME method has been most extensively studied on the map that is compatible with a set of *phased* structure factors, whose phases are already known or assumed (Collins, 1982; Wilkins, Varghese & Lehmann, 1983; Wilkins, 1983; Bricogne, 1984; Wilkins & Stuart, 1986; Gull, Livesey & Sivia, 1987). The primary interest here is in phasing as yet unphased reflections using the Fourier components that the ME map contains in addition to those used in its construction. This 'phase-extension' scheme rests on the belief that the ME map should correspond to the 'true' or a 'more likely' structure. However, this is not guaranteed by theory and remains to be demonstrated with actual crystallographic data (Livesey & Skilling, 1985). Phased ME calculations already carried out for proteins (Collins, 1982; Bricogne, 1984; Wilkins & Stuart, 1986) have shown significant improvements in the interpretability of maps. Although these results tend to indicate that the ME method is effective even at low resolutions, the maximization of entropy in these calculations was largely restricted by prior determination of the phase angles of the basis reflections, which were somewhat arbitrarily chosen. Clearly a different choice of phase angles could lead to a higher-entropy map, which might not necessarily be of good quality.

The above discussion indicates that, in order to examine whether the ME map corresponds to the correct structure, that is to say, whether entropy can be a reliable figure of merit, we need to maximize entropy under *phaseless* constraints to refine phases simultaneously. An immediate choice for such a ME method may be to use a complete set of observed structure-factor amplitudes and to constrain the map to satisfy each of them, *i.e.* $|F_h| - |F_h^{obs}| = 0$. This ME calculation seems to be the most fundamental in crystallography in the sense that the observed data are fully utilized with no assumptions on phases. However, this has not been attempted for the following reasons (Gull & Daniell, 1978; Wilkins, Varghese & Lehmann, 1983; Lemaréchal & Navaza, 1991). (i) Observed data are inevitably noisy and exact fitting of such data would introduce spurious details into the map arising from errors in the data. (ii) The existence of numerous separate constraints results mathematically in a proliferation of Lagrange multipliers and computation of a solution becomes unwieldy in all but the simplest cases. (iii) The ME calculation is expected to have a radius of convergence of the same order as those of other variational techniques such as least-squares refinements. When starting from outside the radius, the least-squares refinements will converge to a local optimum, while the constrained optimization will not always do so but may often diverge. (iv) Finally, when the Lagrangian approach is used, it is difficult to obtain a local maximum with a negative-definite Hessian. These reasons point to the difficulties involved in the ME calculation, but this paper will show that they are not prohibitive for most practical applications. Sjölin, Prince, Svensson & Gilliland (1991) have solved an equivalent ME problem in which trial phase information is assigned in logarithmic space, then members of the corresponding subset of structure moduli are fitted exactly.

0108-7673/92/060842-09$06.00

A way to avoid the difficulties has been proposed (Gull & Daniell, 1978; Wilkins, Varghese & Lehmann, 1983) employing, instead of many individual constraints, a single 'weak' statistical constraint $\sum_{\mathbf{h}}[(|F_{\mathbf{h}}|-|F_{\mathbf{h}}^{\rm obs}|)/\sigma_{\mathbf{h}}]^2 = c, c \leq M$, where M is the number of reflections used. Similar methods have been used in phaseless ME calculations (Bryan, Bansal, Folkhard, Nave & Marvin, 1983; Marvin, Bryan & Nave, 1987; Navaza, 1986). However, since any reduction of constraints may weaken the power of the ME method, such simplifications should be avoided if possible.

Described here is a method developed for calculating the ME map under the 'strong' constraints described above, which includes a simple algorithm that can mostly circumvent the difficulty of divergence. Numerical results are presented, demonstrating (i) how the method works, (ii) what ME maps are like at various resolutions, (iii) what will happen when sharpened data such as unitary structure factors are used and (iv) whether the method can be used to refine structures. Based on these, we discuss the relevance of the ME method to X-ray structure determination.

Method

Consider a unit cell divided into equal pixels, with $\rho_{\mathbf{x}}$ being the average electron density of the pixel located at $\mathbf{x}$. Structure factors are calculated as $F_{\mathbf{h}} = |F_{\mathbf{h}}| \exp(i\varphi_{\mathbf{h}}) = (V/N)\sum_{\mathbf{x}} \rho_{\mathbf{x}} \exp(2\pi i \mathbf{h}\cdot\mathbf{x})$, where V and N denote the cell volume and the number of pixels, respectively. Then find the maximum of a Shannon/Jaynes entropy (Shannon, 1949; Jaynes, 1957) relative to a uniform distribution ($\rho_{\mathbf{x}} = e$),

$$S = -(V/N)\sum_{\mathbf{x}} \rho_{\mathbf{x}} \ln(\rho_{\mathbf{x}}/e), \tag{1}$$

under the constraints

$$g_{\mathbf{h}} = |F_{\mathbf{h}}| - |F_{\mathbf{h}}^{\rm obs}| = 0, \tag{2}$$

where $\mathbf{h}$ comprises the set of reflections used, including 000. If we follow the standard method, this constrained optimization problem may be solved by considering a Lagrangian $L = S + \sum_{\mathbf{h}} \lambda_{\mathbf{h}} g_{\mathbf{h}}$, where $\lambda_{\mathbf{h}}$ are Lagrange multipliers. Solutions to the problem can be obtained as stationary points of the Lagrangian, where $\partial L/\partial \rho_{\mathbf{x}} = 0$ and $\partial L/\partial \lambda_{\mathbf{h}} = 0$. From the former condition, we have

$$\rho_{\mathbf{x}} = \exp\left[\sum_{\mathbf{h}} \lambda_{\mathbf{h}} \exp(i\varphi_{\mathbf{h}}) \exp(-2\pi i \mathbf{h}\cdot\mathbf{x})\right]; \tag{3}$$

the latter simply reduces to (2). We must then solve the nonlinear equations (2) and (3) simultaneously as functions of $\rho_{\mathbf{x}}$ and $\lambda_{\mathbf{h}}$, which is by no means a simple task. According to a constrained minimization method in general use (Hestenes, 1969), solutions to the present problem may alternatively be obtained by minimizing the measure

$$H = -S - \sum_{\mathbf{h}} \lambda_{\mathbf{h}} g_{\mathbf{h}} + (w/2)\sum_{\mathbf{h}} g_{\mathbf{h}}^2, \tag{4}$$

provided the positive constant w is sufficiently large. This minimization may proceed as follows. First, keeping $\lambda_{\mathbf{h}}$ at the current values, minimize H with respect to $\rho_{\mathbf{x}}$. This is done pixelwise by the Newton/Raphson method using the derivatives

$$\frac{N}{V}\frac{\partial H}{\partial \rho_{\mathbf{x}}} = \ln \rho_{\mathbf{x}} - \sum_{\mathbf{h}}[\lambda_{\mathbf{h}} + w(|F_{\mathbf{h}}^{\rm obs}| - |F_{\mathbf{h}}|)] \times \exp(i\varphi_{\mathbf{h}}) \exp(-2\pi i \mathbf{h}\cdot\mathbf{x}) \tag{5}$$

and

$$\frac{N}{V}\frac{\partial^2 H}{\partial \rho_{\mathbf{x}} \partial \rho_{\mathbf{x}'}} = \delta_{\mathbf{x}\mathbf{x}'}(1/\rho_{\mathbf{x}} + w), \tag{6}$$

where the approximation $\rho_{\mathbf{x}} \simeq \sum_{\mathbf{h}} F_{\mathbf{h}} \exp(-2\pi i \mathbf{h}\cdot\mathbf{x})$ is used to obtain the second derivative. Now we have new estimates for $\rho_{\mathbf{x}}$:

$$\rho_{\mathbf{x}}^{\rm new} = \rho_{\mathbf{x}} + [\ln(\rho_{\mathbf{x}}^{\lambda}/\rho_{\mathbf{x}}) + w\Delta\rho_{\mathbf{x}}]/(1/\rho_{\mathbf{x}} + w), \tag{7}$$

where

$$\rho_{\mathbf{x}}^{\lambda} = \exp\left[\sum_{\mathbf{h}} \lambda_{\mathbf{h}} \exp(i\varphi_{\mathbf{h}}) \exp(-2\pi i \mathbf{h}\cdot\mathbf{x})\right] \tag{8}$$

and

$$\Delta\rho_{\mathbf{x}} = \sum_{\mathbf{h}}(|F_{\mathbf{h}}^{\rm obs}| - |F_{\mathbf{h}}|) \exp(i\varphi_{\mathbf{h}}) \exp(-2\pi i \mathbf{h}\cdot\mathbf{x}). \tag{9}$$

It should be noticed that, when updating $\rho_{\mathbf{x}}$, we must also do so with $\varphi_{\mathbf{h}}$. This minimization step is repeated until convergence is obtained.

Next, we update $\lambda_{\mathbf{h}}$ by new estimates that may be obtained by comparing the right-hand side of (5), which must have already vanished in the above minimization, with the following equation which the true solution $(\rho_{\mathbf{x}}, \lambda_{\mathbf{h}}) = (\rho_{\mathbf{x}}^{(0)}, \lambda_{\mathbf{h}}^{(0)})$ should satisfy:

$$\ln \rho_{\mathbf{x}}^{(0)} - \sum_{\mathbf{h}} \lambda_{\mathbf{h}}^{(0)} \exp(i\varphi_{\mathbf{h}}^{(0)}) \exp(-2\pi i \mathbf{h}\cdot\mathbf{x}) = 0, \tag{10}$$

where the phases $\varphi_{\mathbf{h}}^{(0)}$ correspond to $\rho_{\mathbf{x}}^{(0)}$:

$$\lambda_{\mathbf{h}}^{\rm new} = \lambda_{\mathbf{h}} + w(|F_{\mathbf{h}}^{\rm obs}| - |F_{\mathbf{h}}|). \tag{11}$$

The whole process up to this point is then repeated. If the final convergence is obtained, (11) guarantees that $|F_{\mathbf{h}}| = |F_{\mathbf{h}}^{\rm obs}|$. Then (7) shows that $\rho_{\mathbf{x}} = \rho_{\mathbf{x}}^{\lambda}$, which indicates that $\rho_{\mathbf{x}}$ is a ME solution compatible with (3).

This algorithm has several notable features. (i) The term $w\sum_{\mathbf{h}} g_{\mathbf{h}}^2$ in H acts as a penalty function but the final result, in principle, will not depend on the choice of the weight w (Ichikawa, 1975). This feature, however, will be modified by the algorithm used for avoiding the difficulty of divergence, as will be described later. (ii) The

constraints can be exactly satisfied. (iii) Since H explicitly includes the entropy term, the entropy maximization will not stop even when the constraints are exactly satisfied. (iv) Since the algorithm for the constrained minimization is applicable to non-convex functions (Ichikawa, 1975), we can avoid the difficulty in obtaining a true local optimum as encountered when the Lagrangian approach is used (Lemaréchal & Navaza, 1991). (v) All necessary calculations are done by fast Fourier transforms.

Multimodality

As mentioned in the *Introduction*, the ME calculation described above is not always convergent. This difficulty is related to the multimodality of the function H and is best illustrated by a centric reflection whose starting phase has been set incorrectly. Since the phase is constrained to have one of the two discrete values separated by π, it is obvious that the phase cannot be refined continuously, indicating that the initial and final states belong to different branches of the H surface. In such a case, the optimization may fail to bring the structure-factor amplitude of the reflection close to the observed value and, consequently, (11) will accumulate differences, $|F_{\mathbf{h}}^{\rm obs}| - |F_{\mathbf{h}}|$, of successive iterations in its Lagrange multiplier $\lambda_{\mathbf{h}}$, which eventually becomes large enough to give rise to a divergence. This consideration suggests a simple method for dealing with the divergence that uses the magnitude of $\lambda_{\mathbf{h}}$ as an indicator for an incorrect phase: those reflections for which $|\lambda_{\mathbf{h}}|/|F_{\mathbf{h}}^{\rm obs}|$ is larger than a given threshold are excluded from the data set and, sometime later, are included again. This exclusion/inclusion algorithm introduces a discontinuity into the optimization and may facilitate the optimization path to switch to a nearby branch of H, which may be more preferable with respect to entropy, since, during the exclusion, the entropy term is dominant in H to some extent. The multimodality may not be specific to centric reflections but there must be acentric ones whose phases cannot be refined continuously. Therefore, the algorithm should be applied to every reflection in the data set.

The threshold must be set at a sufficiently high value, otherwise most of the reflections will be excluded from the data set, leaving the optimization meaningless. Likewise, starting phases have to be reasonably correct so that a substantial number of reflections can be used for the optimization.

With this algorithm, the present method acquires some capabilities for exploring a region wider than the usual radius of convergence. However, the optimization, in general, will be trapped at local optima. Regarding this, the choice of the weight w in H plays a unique role; when we use a smaller value for it, the constraints $g_{\mathbf{h}}$ are less satisfied at initial stages of optimization and, consequently, the exclusion/inclusion algorithm will more often be invoked to change the search path to a branch of higher entropy. Therefore, the optimization is more likely to converge to a local optimum of higher entropy. On the other hand, a trial with a larger w tends to follow a path along which the constraints are satisfied more closely. Therefore, once the constraints are well satisfied, it would be rather difficult to jump to a branch of higher entropy.

Implementation

(a) Setting up the initial densities and Lagrange multipliers

The initial densities $\rho_{\mathbf{x}}$ are calculated using a given starting set of phases, $\psi_{\mathbf{h}}$, and their observed structure-factor amplitudes as usual. Often some of the densities are negative or too small to evaluate $1/\rho_{\mathbf{x}}$ in (7) and hence they must be regularized: $\rho_{\mathbf{x}} \geq 10^{-4}$ e Å^{-3}. This regularization is also used in subsequent calculations. The initial Lagrange multipliers $\lambda_{\mathbf{h}}$ are calculated from $\rho_{\mathbf{x}}$ using (3) as

$$\lambda_{\mathbf{h}} = (V/N)\mathrm{Re}\left[\exp(-i\psi_{\mathbf{h}})\sum_{\mathbf{x}} \ln \rho_{\mathbf{x}} \exp(2\pi i \mathbf{h}\cdot\mathbf{x})\right].$$

The estimates are necessarily crude because (3) applies only to the ME densities.

(b) Phase-constrained ME calculation to refine the initials

Before starting the phaseless (*i.e.* phase-unconstrained) ME calculation, we refine the initial densities and multipliers by a ME calculation using the constraints

$$\mathrm{Re}[F_{\mathbf{h}}\exp(-i\psi_{\mathbf{h}})] - |F_{\mathbf{h}}^{\rm obs}| = 0,$$

each of which is one of the two constraints for a phased structure factor; the other constraint that we ignore is $\mathrm{Im}[F_{\mathbf{h}}\exp(-i\psi_{\mathbf{h}})] = 0$ (Bricogne, 1984). This ME calculation can be done in the same way as in the following phase-unconstrained case; (7), (8), (9) and (11) can be used if $\varphi_{\mathbf{h}}$ and $|F_{\mathbf{h}}|$ in these equations are now understood to be $\psi_{\mathbf{h}}$ and $\mathrm{Re}[F_{\mathbf{h}}\exp(-i\psi_{\mathbf{h}})]$, respectively. The other details are the same as in the phase-unconstrained ME calculation. Usually ten iterations (see below) are sufficient to proceed further.

(c) Phase-unconstrained ME calculation

The starting densities and Lagrange multipliers are taken from the above calculation. The update of $\rho_{\mathbf{x}}$ by (7) is to be repeated at most five times if shifts of $\rho_{\mathbf{x}}$ are larger than 10^{-5}. Rigorous convergence of this step is not always required to update $\lambda_{\mathbf{h}}$ by (11). With the process until the updating of $\lambda_{\mathbf{h}}$ being defined as one iteration, 300 iterations were performed in the following numerical calculations.

(d) Exclusion/inclusion of incorrect reflections

The exclusion/inclusion algorithm already described is used in the phase-unconstrained ME calculation: those reflections with $|\lambda_{\mathbf{h}}|/|F_{\mathbf{h}}^{\rm obs}| > 10$ are excluded from the data set and then included again with $\lambda_{\mathbf{h}} = 0$ when their calculated structure factors fall in the range $0.5 < |F_{\mathbf{h}}|/|F_{\mathbf{h}}^{\rm obs}| < 1.5$. In preliminary runs, the algorithm seemed to be effective not only for dealing with the multimodality but also for eliminating erroneous measurements. However, in some cases where the data set used was small,

we found that several significant reflections remained excluded from the data set to the end of the optimization and, at the same time, entropy rose much higher than otherwise. Since this made it difficult to compare the entropies of different trials, the algorithm was used only in the first 100 iterations and, in the remaining 200 iterations, all reflections in the data set were always used, although this caused some trials to be divergent.

(e) Dumping

At the initial stages of the optimization, in both the phase-constrained and phase-unconstrained cases, errors in $\lambda_{\mathbf{h}}$ are biased by the exponential function of (8), leading to absurd $\rho_{\mathbf{x}}^{\lambda}$ values. Therefore, we restrict them in the range $10^{-4} \leq \rho_{\mathbf{x}}^{\lambda} \leq 10^{3}$. However, no attempts are made to restrict $\lambda_{\mathbf{h}}$ themselves.

(f) Statistics

The following values are calculated during and after the calculation.

$$R = \sum_{\mathbf{h}} ||F_{\mathbf{h}}| - |F_{\mathbf{h}}^{\mathrm{obs}}|| \Big/ \sum_{\mathbf{h}} |F_{\mathbf{h}}^{\mathrm{obs}}|,$$

$$R(\rho_{\mathbf{x}}, \rho_{\mathbf{x}}^{\lambda}) = \sum_{\mathbf{x}} |\rho_{\mathbf{x}}^{\lambda} - \rho_{\mathbf{x}}| \Big/ \sum_{\mathbf{x}} |\rho_{\mathbf{x}}|,$$

$$S^{0} = -\sum_{\mathbf{x}} p_{\mathbf{x}} \ln p_{\mathbf{x}},$$

where $p_{\mathbf{x}} = \rho_{\mathbf{x}} / \sum_{\mathbf{x}} \rho_{\mathbf{x}}$. The $R(\rho_{\mathbf{x}}, \rho_{\mathbf{x}}^{\lambda})$ factor measures to what extent the constrained optimization has been achieved as it goes to zero at the optimum. The normalized entropy S^{0} is linearly related to S in (1).

(g) Computer program

The algorithm was programmed as a module in the program system *Xtal*3.0 (Hall & Stuart, 1990). The essential part of our back-Fourier-transform routine was adopted from *RFOURR*, which was coded by Collins, Stewart & Holden (1990) and uses a set of Winograd Fourier-transform subroutines (Silverman, 1977). A corresponding forward-Fourier-transform routine was written after the method given by Ten Eyck (1985). All necessary data are stored in the core and no disk access is done during the iterations. Each run of the following calculations took a CPU time of 5–6 h on a VAX VS3100 workstation.

Numerical calculations

In order to examine how the present algorithm works and to study how the phaseless ME optimization affects the estimation of electron densities, numerical calculations were done using the data observed with 2′-deoxyadenosine (I) (Sato, 1984).

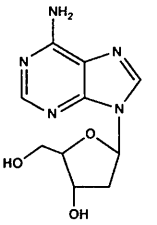

(I)

Crystal data: $C_{10}H_{13}N_5O_3$, monoclinic, $P2_1$, a = 11.298(2), b = 10.393(2), c = 4.819(1) Å, β = 101.51(2)°, V = 554.5(2) Å^3, Z = 2, $F(000)$ = 264, Mo $K\alpha$ radiation, 2549 unique reflections measured ($2\theta \leq 70°$; $\sin\theta/\lambda \leq 0.807$ Å^{-1}), R = 0.038 for 2224 observed reflections [$I \geq 2\sigma(I)$].

The same data set as that used in the least-squares refinements was used with the scale factor obtained from the refinements. The pixel size was set to about 0.25 Å (45 × 42 × 20 pixels) and the optimization was started from the least-squares phases.

First, we examined the effects due to the choice of w, the weight for the contribution from the constraints (nos. 1–5 in Table 1). Final convergence was obtained with w larger than 5.0, although the convergence became slower as w increased. The constraints (1) were exactly satisfied up to R = 0.0000 and this was common to all the calculations presented in this study. On the other hand, $R(\rho_{\mathbf{x}}, \rho_{\mathbf{x}}^{\lambda})$, a measure that represents to what extent the constrained optimization has been achieved, showed a slight increase as w increased. This is probably due to numerical round-off errors involved in estimating (11). The Langrange multipliers were generally small: for example, with solution 2, only 11 out of 2224 used reflections had $|\lambda_{\mathbf{h}}|/|F_{\mathbf{h}}^{\mathrm{obs}}| > 3.0$ with the highest being 6.8.

We have obtained four solutions with w in the range 5.0–40.0, among which three can be considered to be different: (i) solutions 4 and 5 are essentially the same because the $F_{\mathbf{h}}$-weighted mean phase difference, $\langle|\Delta\varphi_{\mathbf{h}}|\rangle \equiv \sum_{\mathbf{h}} |F_{\mathbf{h}}^{\mathrm{obs}}||\Delta\varphi_{\mathbf{h}}| / \sum_{\mathbf{h}} |F_{\mathbf{h}}^{\mathrm{obs}}|$, is 0.17°; (ii) all the centric reflections in solutions 4 and 5 have the same phase angles as those obtained by the least-squares refinements, while a weak centric reflection 600 underwent a phase change of π with nos. 2 and 3, showing that the two sets of solutions belong to different branches of H; and (iii) it is not quite clear whether solutions 2 and 3 belong to different local optima well separated from each other but we assume so because $\langle|\Delta\varphi_{\mathbf{h}}|\rangle$ between them is not small (0.84°).

Despite their differences in phases and entropies, all the ME maps thus obtained turned out to be almost the same. This is because the differences arose primarily from weak, less-significant, reflections: $\langle|\Delta\varphi_{\mathbf{h}}|\rangle$ between solutions 2 and 5, for example, is 0.57° for 59 strong reflections with $|F_{\mathbf{h}}^{\mathrm{obs}}| > 20$, which is compared to 2.1° for 636 weak reflections with $|F_{\mathbf{h}}^{\mathrm{obs}}| < 2$. Therefore, even if a 'dominating structure' exists, the ME optimization with the strong

Table 1. *Statistics of phaseless ME calculations*

No.	F_h/U_h	$\langle B \rangle$ (Å^2)	w	S^0	$R(\rho_x, \rho_x^\lambda)$	$\langle \lvert\Delta\varphi_h\rvert \rangle$ (°)†	Fig.
(*A*) 0.62 Å resolution, sin $\theta/\lambda \le 0.807$ Å^{-1}, 2224 reflections							
1	F_h	2.0	2.5	Oscillates	-	-	
2			5.0	9.3356	0.0005	3.2	
3			10.0	9.3355	0.0006	2.9	1(*b*)
4			20.0	9.3349	0.0009	2.7	
5			40.0	9.3348	0.0018	2.7	
6*			10.0	9.3356	0.0008	2.9	
(*B*) 1.0 Å resolution, sin $\theta/\lambda \le 0.500$ Å^{-1}, 620 reflections							
7	F_h	8.0	10.0	9.7727	0.0001	16	3(*a*)
8			20.0	9.7623	0.0002	8.7	
9		0.0	10.0	9.0726	0.0002	2.9	3(*b*)
10*			10.0	9.0717	0.0011	2.8	
(*C*) 1.5 Å resolution, sin $\theta/\lambda \le 0.325$ Å^{-1}, 175 reflections							
11	F_h	15.0	10.0	10.0347	0.0001	38	2(*b*)
12			20.0	10.0335	0.0027	34	
13		0.0	10.0	9.2556	0.0001	14	4(*a*)
14*			10.0	9.1949	0.0004	20	
15	U_h	6.0	10.0	8.4826	0.0002	6.8	4(*b*)
16*				8.4827	0.0009	6.8	
(*D*) 2.0 Å resolution, sin $\theta/\lambda \le 0.250$ Å^{-1}, 86 reflections							
17	U_h	4.0	10.0	8.5103	0.0002	19	5(*a*)
18*				8.6846	0.0009	41	5(*b*)

*Started from the phases calculated from a partial structure.
†The weighted mean phase difference compared with the least-squares phases.

constraints will give many solutions of similar entropies, which differ only in the phases of less-significant reflections. Although this feature might have arisen partly from exact fitting of erroneous weak measurements, it will not pose practical difficulties.

A representative ME map (Fig. 1*b*) corresponding to solution 3 is markedly different from the conventional Fourier map (Fig. 1*a*) calculated with the least-squares phases, despite the small differences in phases ($\langle \lvert\Delta\varphi_h\rvert \rangle = 3.7°$). (i) Its background is everywhere positive ($\rho_x \ge 0.002$) and smooth. (ii) The peak heights of non-H atoms are 1.2–1.6 times higher than those of the usual Fourier map and it seems that larger peaks in the latter have been more enhanced. (iii) On the other hand, it seems that weak densities have been rather smeared out. Indeed, none of the H atoms are resolved.

Low-resolution structures

In order to examine how the ME optimization affects low-resolution structures, calculations were carried out by modifying the observed structure factors as $\lvert F_h^{obs}\rvert \exp(-B_{add} s^2)$, where $s = \sin\theta/\lambda$. Since the Wilson plot gave $B = 2.0$ Å^2 with the original data, $\langle B \rangle$ [$\langle B \rangle \equiv (B_{add} + 2.0)$ Å^2] stands for the overall temperature factor.

(*a*) 1.0 Å *resolution*. We used 620 reflections ($s \le 0.500$ Å^{-1}) in ME calculations on a structure with $\langle B \rangle = 8.0$ Å^2, a value typical of the structures of this resolution. Again we obtained several solutions (nos. 7–8 in Table 1), among which the one with the highest entropy had phase angles somewhat different from the least-squares ones ($\langle \lvert\Delta\varphi_h\rvert \rangle = 16°$). Although its ME map (Fig. 3*a*) is interpretable, such density enhancement at the atomic centers as observed with the high-resolution structure no longer took place.

(*b*) 1.5 Å *resolution*. Similar calculations were done for a structure with $\langle B \rangle = 15.0$ Å^2. In this case, 175 reflections with $s \le 0.325$ Å^{-1} were used (nos. 11–12 in Table 1). The phase angles of the solution of the highest entropy were now quite different from the least-squares ones, $\langle \lvert\Delta\varphi_h\rvert \rangle$ being 38°. Accordingly, its ME map (Fig. 2*b*) shows sizable deteriorations when compared to the corresponding conventional Fourier map (Fig. 2*a*): (i) the densities of small portions of the adenine ring have abnormally evolved and (ii) the molecular boundary has been obscured.

The conclusion reached from these calculations together with those of the last section is that the ME maps are not the real or correct representation of electron densities but are subject to substantial deformations. At resolutions where individual atoms are resolved, the deformation takes place most noticeably at atomic centers, where the densities are enhanced. However, it should be noticed that this enhancement by itself is not favored by entropy. Rather, the entropy is primarily concerned at these atomic resolutions to make the densities positive and smooth by adding unobserved higher Fourier components to them; the density enhancement that we have seen in the ME map is probably a consequence of this action. It is for the same reason that phased ME calculations always make peaks sharp (*e.g.* Bricogne, 1984). On the other hand, at lower resolutions where only atomic groups rather than individual atoms are recognizable, the density deformation takes place in a different way: the atomic groups are not emphasized as a whole but only small portions of them are enhanced. At these resolutions, since the positivity of densities is easy to fulfil, entropy will reduce a region of

higher densities. It seems that a majority of higher densities are lowered at the expense of small portions of enhanced higher densities. This deformation deteriorates the estimates of phases.

Use of sharpened data

It is customary in direct methods to use unitary structure factors $U_{\mathbf{h}}$ or normalized structure factors $E_{\mathbf{h}}$ instead of usual structure factors (Woolfson, 1987). This is primarily for mathematical convenience to make various probabilistic calculations feasible but it is possible that the use of such sharpened structure factors helps the direct methods to work. With this in mind, we have tried the ME optimization using sharpened data.

(*a*) 1.0 Å *resolution*. First, we carried out ME calculations with the 1.0 Å data on a structure for which $\langle B \rangle = 0.0\,\text{Å}^2$ (no. 9 in Table 1). This trial is equivalent to doing the same calculation as that in the last section but with the observed structure factors sharpened by $\exp(8.0s^2)$. In this case, the densities at the atomic centers have been significantly enhanced (Fig. 3*b*) and, accordingly, the obtained phases are now remarkably close to the least-squares ones ($\langle|\Delta\varphi_{\mathbf{h}}|\rangle = 2.9°$).

(*b*) 1.5 Å *resolution*. Similar calculations were carried out with the 1.5 Å data (no. 15 in Table 1). The obtained ME map (Fig. 4*a*) again shows significant improvement

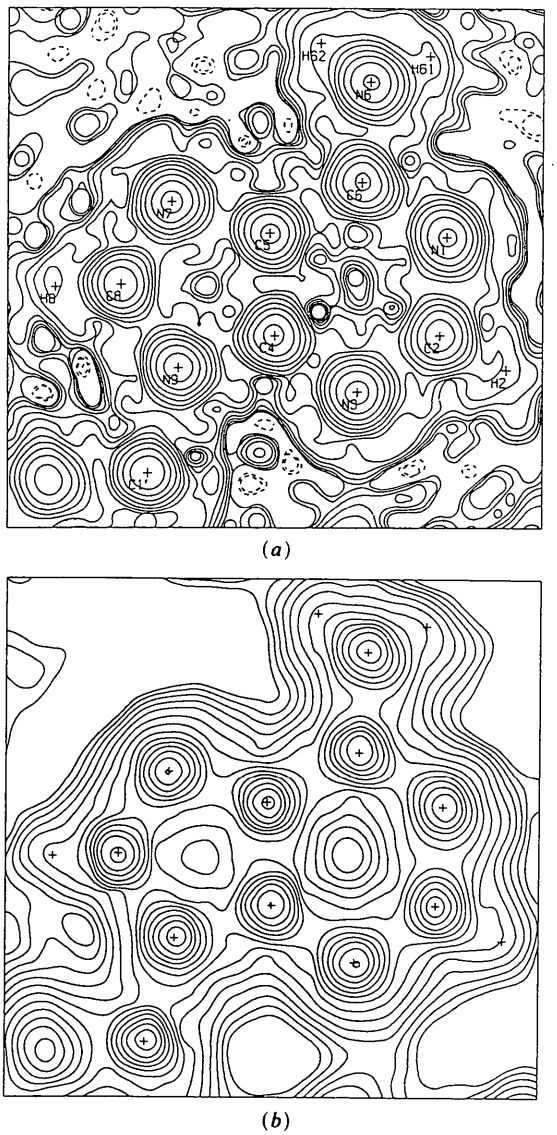

Fig. 1. 0.62 Å resolution electron densities in the plane of the adenine ring of 2′-deoxyadenosine. (*a*) Conventional Fourier density map calculated with the least-squares phases; (*b*) corresponding ME density map. Contours were drawn at the levels $\pm 0.1 \times 1.5^n$ e Å^{-3}; positive contours solid; negative dashed. The figures were drawn using *Xtal*3.0 (Hall & Stewart, 1990).

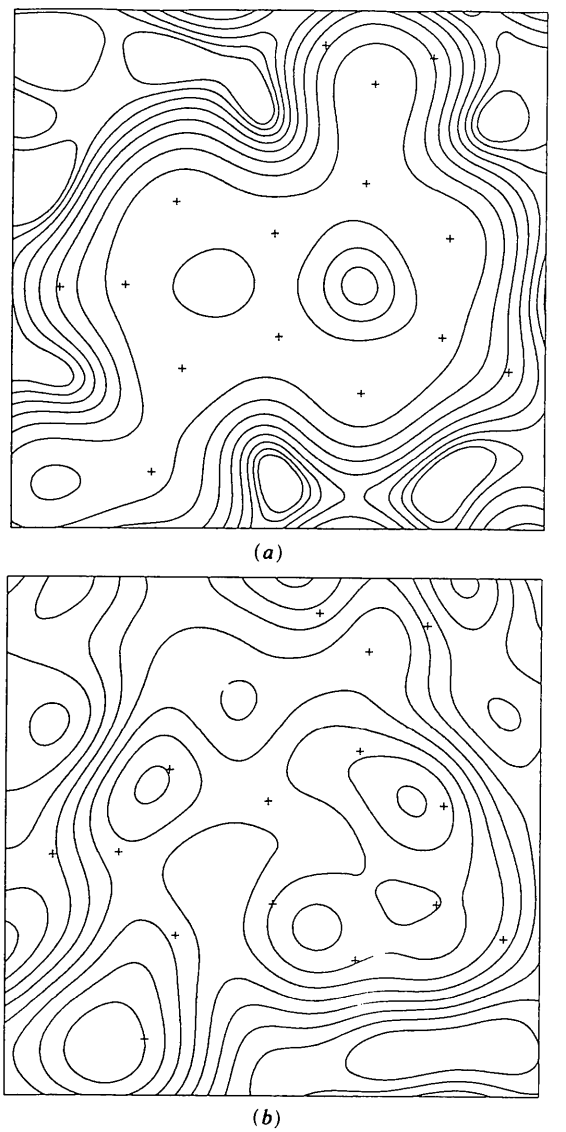

Fig. 2. 1.5 Å resolution electron densities. (*a*) Conventional Fourier density map calculated as described in Fig. 1(*a*) but with the overall temperature factor $\langle B \rangle = 15.0\,\text{Å}^2$; (*b*) corresponding ME density map. For other details, see Fig. 1.

in interpretability compared with the corresponding ME map (Fig. 2*b*), which was obtained with unsharpened structure factors. However, as the phases are not as close to the least-squares ones ($\langle|\Delta\varphi_{\mathbf{h}}|\rangle = 14°$), the centering of densities on the atomic centers is moderate.

(*c*) *Use of unitary structure factors*; 1.5 Å *resolution*. Next, we attempted to use unitary structure factors. However, since the densities corresponding to point atoms were too abrupt to do realistic calculations, it was necessary to blur the unitary structure factors as $|U_{\mathbf{h}}^{\text{obs}}|\exp(-\langle B\rangle s^2)$ (when $U_{\mathbf{h}}$ is used, the symbol $\langle B\rangle$ is used with this meaning). It was also necessary to attenuate shifts of $\lambda_{\mathbf{h}}$ for high-angle reflections. This was done by applying an attenuating factor $\exp(-B_{\text{att}}s^2)$ to w in (11), B_{att} being chosen so that the factor is 1/4 at the upper limit of s for the data used. ME calculations were done with the 1.5 Å $U_{\mathbf{h}}$ data blurred by $\langle B\rangle = 6.0$ Å^2 (no. 15 in Table 1). The obtained ME map is shown in Fig. 4(*b*). Now all the atomic sites are clearly visible, although some of them are slightly misplaced. Accordingly, the phases are nearly correct ($\langle|\Delta\varphi_{\mathbf{h}}|\rangle = 6.8°$).

(*d*) 2.0 Å *resolution*. Similar calculations were made with 2.0 Å $U_{\mathbf{h}}$ data (86 reflections) blurred by $\langle B\rangle = 4.0$ Å^2 (no. 17 in Table 1). The obtained ME map (Fig. 5*a*) is interpretable to a large extent but the phases are not so correct ($\langle|\Delta\varphi_{\mathbf{h}}|\rangle = 14°$).

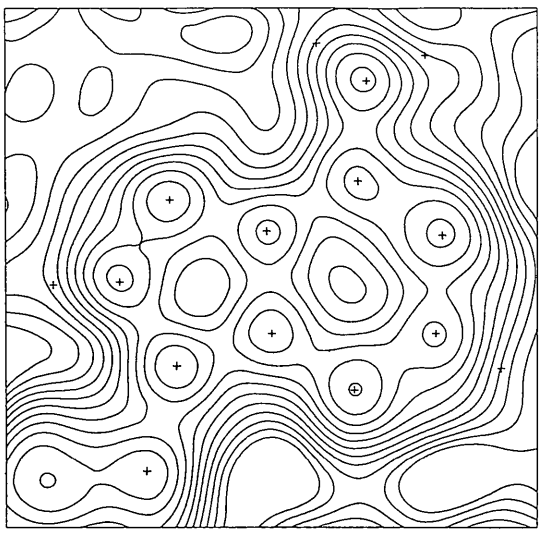

(*a*)

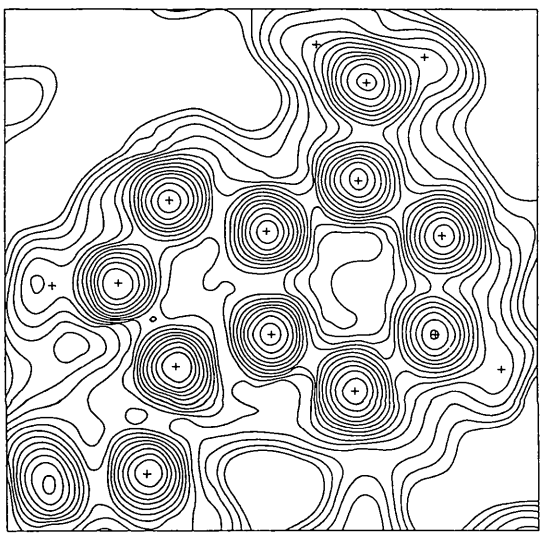

(*b*)

Fig. 3. 1.0 Å resolution electron densities. (*a*) ME density map corresponding to a structure with $\langle B\rangle = 8.0$ Å^2; (*b*) ME density map corresponding to a structure with $\langle B\rangle = 0.0$ Å^2. These figures demonstrate that the use of sharpened structure factors effectively increases the resolution of the ME map. For other details, see Fig. 1.

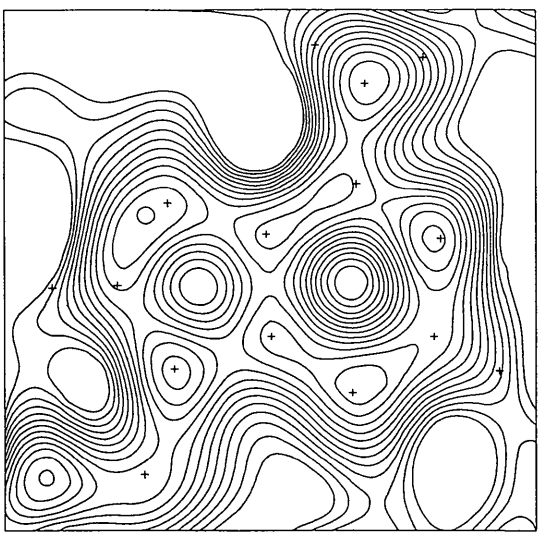

(*a*)

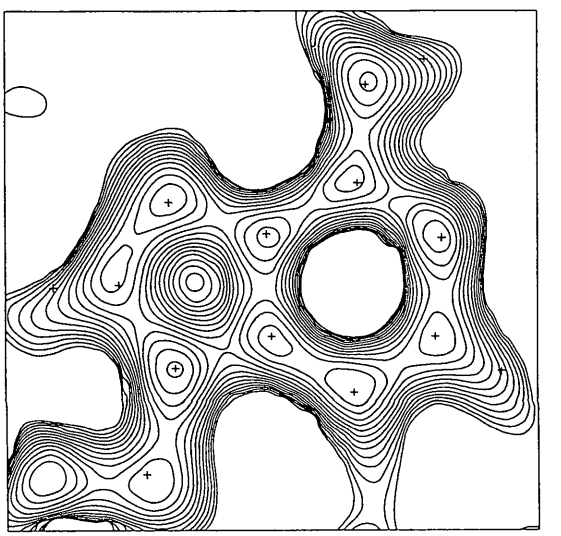

(*b*)

Fig. 4. 1.5 Å resolution electron densities. (*a*) ME density map corresponding to a structure with $\langle B\rangle = 0.0$ Å^2; (*b*) ME density map calculated with $|U_{\mathbf{h}}^{\text{obs}}|\exp(-6.0s^2)$. These figures demonstrate how the use of sharpened structure factors affects 1.5 Å ME densities in two different ways. For other details, see Fig. 1.

As envisaged in the beginning, the use of sharpened structure factors did indeed enhance the phasing power of the ME method. However, we do not expect that we can go much further with this technique. Indeed, it was possible to obtain ME solutions with $|U_{\mathbf{h}}^{\rm obs}|$ not blurred when the resolution of the data was lower than 2.5 Å (46 reflections or less) but none of the solutions were interpretable or of atomic resolution. This indicates that (i) even if there were to exist a local optimum corresponding to the correct structure, its entropy could not be higher than those of the meaningless solutions and (ii) the use of unitary structure factors does not ensure the point-atomic resolution of densities.

Structure refinements

Thus far, the ME calculations have always started from the correct least-squares phases. Now let us examine whether the present algorithm has the capability of heuristic searching in structure determination. The algorithm is not well suited for doing *ab initio* structure determination so what we are going to attempt is to obtain the correct structure by starting from a partial structure, which consists of the 14 skeletal atoms of the two rings of 2′-deoxyadenosine, about 3/4 of the whole molecule. The structure gave $R = 0.29$ and the starting phases calculated from it deviated from the correct ones by, for example, $\langle|\Delta\varphi_{\mathbf{h}}|\rangle = 29°$ for the 1.5 Å data.

This problem would be trivial if we applied successive Fourier refinements to high-resolution data. Yet it is worthwhile trying it for the following reasons: (i) even with the Fourier technique, structure refinements would not be so trivial when data are of resolution as low as 1.5 Å because reconstruction of a structure in terms of atomic models, as required by the technique, is not always straightforward at these resolutions; (ii) in view of variational calculations, it is worthwhile trying the problem because the starting phases of 19 centric reflections ($s \leq 0.807$ Å^{-1}) have to be changed to reach the correct solution; and (iii) the trial should provide some information as to what extent the optimum solutions obtained in the last three sections are dominant in a wider domain.

We succeeded in recovering the 'correct' structures corresponding to Figs. 1(*b*), 3(*b*) and 4(*b*) (the results are listed as nos. 6, 10 and 16 in Table 1, respectively). This indicates that the entropy of each of these structures dominates the domain to the extent that all necessary branchings take place through the exclusion/inclusion algorithm. On the other hand, a trial corresponding to Fig. 4(*a*) converged to a local optimum of lower entropy (no. 14 in Table 1), indicating that the domination of the 'correct' solution is not sufficient. Although the obtained ME map (not shown) is still interpretable, one of the atoms (C1′) is appreciably misplaced.

Another situation was revealed when we did a calculation corresponding to the 2.0 Å structure (Fig. 5*a*), which was obtained by using $|U_{\mathbf{h}}^{\rm obs}|$ blurred by $\langle B\rangle = 4.0$ Å^2. The ME structure now obtained (no. 18 in Table 1; Fig. 5*b*) has an entropy much higher than that of the other interpretable solution but is utterly meaningless. It should be noted that the 'correct' solution contains three reflections with $|\lambda_{\mathbf{h}}|/|F_{\mathbf{h}}^{\rm obs}| > 10$, while none of the reflections used with the other, meaningless, solution have a value larger than 7. It seems, therefore, that a solution of lower entropy involves larger Lagrange multipliers.

Interestingly, in the successful cases the density enhancement at atomic sites always takes place, while this is not so in the unsuccessful cases. Therefore, it seems that the enhancement indeed helps the entropy of the 'correct' structure to be discriminating.

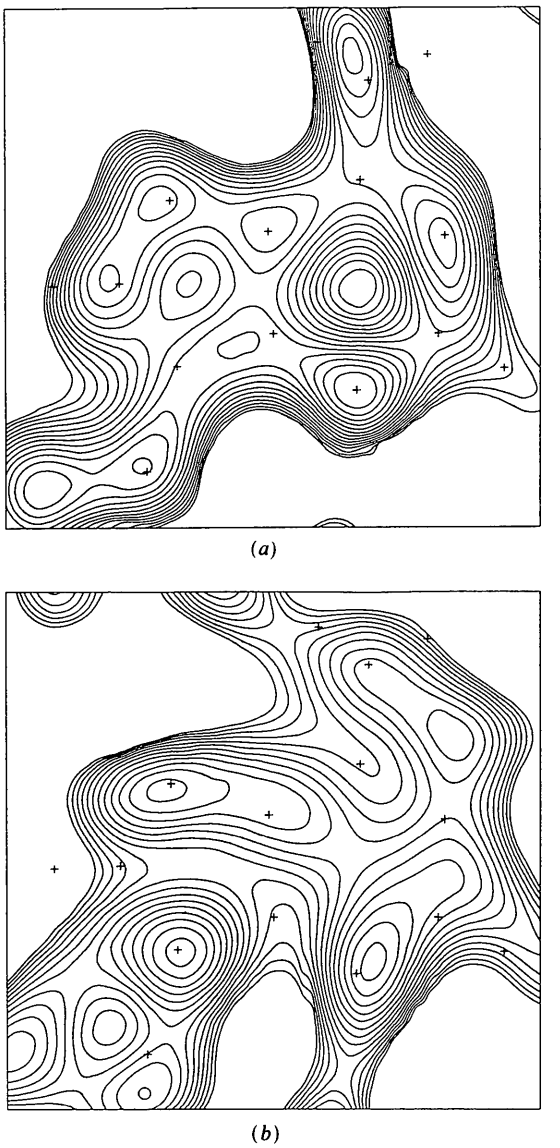

Fig. 5. 2.0 Å resolution electron densities. (*a*) ME density map obtained with $|U_{\mathbf{h}}^{\rm obs}|\exp(-4.0s^2)$ by starting from the least-squares phases; (*b*) ME density map obtained in the same way but now starting from the phases calculated from a partial structure. Note that the latter has a higher entropy than the former but is not interpretable. For other details, see Fig. 1.

Discussion

We have seen that the ME optimization by no means points to the real or correct representation of electron densities but that the densities are subject to substantial deformations. However, the phases of the reflections used are kept close to the correct ones when the resolution of observed data is high enough to resolve individual atoms. This is because, at these resolutions, the deformation takes place primarily at atomic centers, where the densities are significantly enhanced. It is probable that this deformation, in turn, helps the entropy of the structure to dominate over the other local optima, the domination being the major source of power for driving phases to the correct ones. On the other hand, at lower resolutions where only atomic groups rather than individual atoms are recognizable, the ME optimization causes deterioration of the estimates of both densities and phases.

When sharpened structure factors rather than the usual structure factors are used, the resolution of ME maps is effectively increased and, accordingly, the phasing power of the ME method is increased. With this technique, we have succeeded in obtaining the correct atomic structure even with 1.5 Å data. Also it should be noted that, where the ME method is effective, the obtained phases are much more accurate than those obtained by currently available direct methods. These results strongly suggest that the ME method is more effective than direct methods.

We have demonstrated that entropy can be used as a reliable figure of merit for structures whose resolution is higher than 1.5 Å, provided observed structure-factor amplitudes are sharpened. On the other hand, we have seen that the ME method is rarely effective for structures of resolution lower than 2 Å. Nevertheless, there is a possibility that the method might work differently when applied to the structure of macromolecules. This is because a large amount of solvent specific to such structures constitutes a wide background, which would pose additional restrictions on the phases (Wang, 1985). A test *ab initio* ME calculation on a protein by Sjölin, Prince, Svensson & Gilliland (1991) led to an essentially correct structure but the polypeptide chain had been broken up into fragments. A similar fragmentation resulted with a phaseless ME calculation on a virus structure (Marvin, Bryan & Nave, 1987). These deteriorations are probably of the same nature as those found with the low-resolution ME structures obtained in the present study. In such situations, the ME method might be of limited use.

The various features we have found with the ME optimization bear close resemblance to those of direct methods. It has been argued that the ME method, in fact, is a more rigorous extension to the current probabilistic direct methods on the basis of probability theory (Wilkins, Varghese & Lehmann, 1983; Bricogne, 1984; Livesey & Skilling, 1985). If the ME method has indeed captured the essential aspects of direct methods, the present results should give some answers to questions such as why the methods do not work with low-resolution structures and so on.

The ME method is a kind of variational density-modification technique (Navaza, Castellano & Tsoucaris, 1983; Collins & Mahar, 1983; Main, 1990). Such calculations are becoming increasingly feasible with the availability of fast computers. The primary interest here is in obtaining interpretable density maps out of less-interpretable ones without manual intervention. One of the difficulties in these calculations is that all practical trials start from outside the radius of convergence. Our exclusion/inclusion algorithm provides a useful means for it and the present alogrithm adopted for the constrained optimization may be used for evaluation functions other than entropy.

References

BRICOGNE, G. (1984). *Acta Cryst* A**40**, 410-445.

BRYAN, R. K., BANSAL, M., FOLKHARD, W., NAVE, C. & MARVIN, D. A. (1983). *Proc Natl Acad Sci USA*, **80**, 4728-4731.

COLLINS, D. M. (1982). *Nature (London)*, **298**, 49-51.

COLLINS, D. M. & MAHAR, M. C. (1983). *Acta Cryst* A**39**, 252-256.

COLLINS, D. M., STEWART, J. M. & HOLDEN, J. (1990). *RFOURR, Xtal*3.0 *Reference Manual*, edited by S. R. HALL & J. M. STEWART Univs. of Western Australia, Australia, and Maryland, USA.

GULL, S. F. & DANIELL, G. J. (1978). *Nature (London)*, **272**, 686-690.

GULL, S. F., LIVESEY, A. K. & SIVIA, D. S. (1987). *Acta Cryst* A**43**, 112-117.

HALL, S. R. & STEWART, J. M. (1990). Editors. *Xtal*3.0 *Reference Manual* Univs. of Western Australia, Australia, and Maryland, USA.

HESTENES, M. R. (1969). *J Optim Theor Appl* **4**, 303-320.

ICHIKAWA, K. (1975). *SICE Trans.* **11**, 180-186 (in Japanese).

JAYNES, E. T. (1957). *Phys Rev* **106**, 620-630.

LEMARÉCHAL, C. & NAVAZA, J. (1991). *Acta Cryst* A**47**, 631-632.

LIVESEY, A. L. & SKILLING, J. (1985). *Acta Cryst.* A**41**, 113-122.

MAIN, P. (1990). *Acta Cryst* A**46**, 372-377.

MARVIN, D. A., BRYAN, R. K. & NAVE, C. (1987). *J Mol Biol* **193**, 315-343.

NAVAZA, J. (1986). *Acta Cryst* A**42**, 212-223.

NAVAZA, J., CASTELLANO, E. E. & TSOUCARIS, G. (1983). *Acta Cryst* A**39**, 622-631.

SATO, T. (1984). *Acta Cryst* C**40**, 880-882.

SHANNON, C. E. (1949). *Proc Inst Radio Eng NY*, **37**, 10-21.

SHELDRICK, G. M. (1990). *Acta Cryst* A**46**, 467-473.

SILVERMAN, H. K. (1977). *IEEE Trans Acoust Speech Signal Process* **25**, 152-165.

SJÖLIN, L., PRINCE, E., SVENSSON, L. A. & GILLILAND, G. L. (1991). *Acta Cryst* A**47**, 216-223.

TEN EYCK, L. F. (1985). *Methods Enzymol* **115**, 324-337.

WANG, B.-C. (1985). *Methods Enzymol.* **115**, 90-112.

WILKINS, S. W. (1983). *Acta Cryst.* A**39**, 892-896.

WILKINS, S. W. & STUART, D. (1986). *Acta Cryst.* A**42**, 197-202.

WILKINS, S. W., VARGHESE, J. N. & LEHMANN, M. S. (1983). *Acta Cryst.* A**39**, 47-60.

WOOLFSON, M. M. (1987). *Acta Cryst.* A**43**, 593-612.